Supplementary

S2.10.1-1

The calculation of the continuous wavelet transform (CWT) adopts the Morlet wavelet as the basis function. An appropriate frequency resolution is set, with the number of scales per octave (*VoicePerOctave*) set to 32, and the total number of scales for CWT is 287. The calculation formula is shown in Equation (3), where $f_{\max}$ is 500 Hz and $f_{\min}$ is 1 Hz:

$$num\_scales = VoicePerOctave \times log_2 \frac{f_{max}}{f_{min}} \tag{3}$$

Based on the CWT analysis results, the sEMG energy frequency bands are divided into five parts: 0–20 Hz, 20–60 Hz, 60–90 Hz, 90–150 Hz, and 150–500 Hz. The calculation method for the energy of each frequency band is shown in Equation (4) [1]:

$$band\_energy_{a-b} = \frac{1}{\sum WT\_instensity}\left(\sum_{t=1}^{length(signal)} \sum_{f=band\_freq_a}^{band\_freq_b} WT\_instensity_f \right. \tag{4}$$

where *WT_intensity* denotes the total wavelet transform intensity, length(signal) is the length of the sEMG signal, *band_freqa* and *band_freqb* are the start and end frequencies of the target band, respectively, and $WT\_intensity_f$ is the wavelet transform intensity at frequency *f*.

S2.10.1-2

During the entire fatigue-inducing process, the sEMG signal is evenly divided into three segments. The median frequency (MDF) of each segment is calculated separately, and the slope of the three MDF values is fitted. The linear fitting equation is shown in Equation (5). The least squares method is used to linearly fit the MDF values corresponding to the midpoints of the extracted three segments. The calculation method of the residual sum of squares (RSS) is shown in Equation (6), where $segment\_midpoint_i$ is the middle time point of each segment and MDF_i is the *MDF* value at the corresponding time point.

$$y = p_1 x + p_2 \tag{5}$$

$$RSS = \sum_{i=1}^{3} (MDF_i - (p_1\ segment\_midpiont_i + p_2))^2 \tag{6}$$

where MDF_i is the actual *MDF* value and $p_1 segment\_midpiont_i + p_2$ is the fitted value [2].

S2.10.1-3

The root mean square (RMS) of each sEMG signal is calculated as shown in Equation (7), where length(signal) is the length of the signal and $collection\_value_i^2$ is the collected value of the signal [3, 4]:

$$RMS = \sqrt{\frac{1}{length(signal)} \sum_{i=1}^{length(signal)} collection\_value_i^2} \tag{7}$$

Figure S1

Joint angles obtained by inverse kinematics under three postures: (a) quiet standing, (b) left lateral bridge, and (c) left bird-dog. Each group of figures shows the lumbar angular displacement (deg) of bending, flexion, and rotation between intervertebral discs (*IVD*)

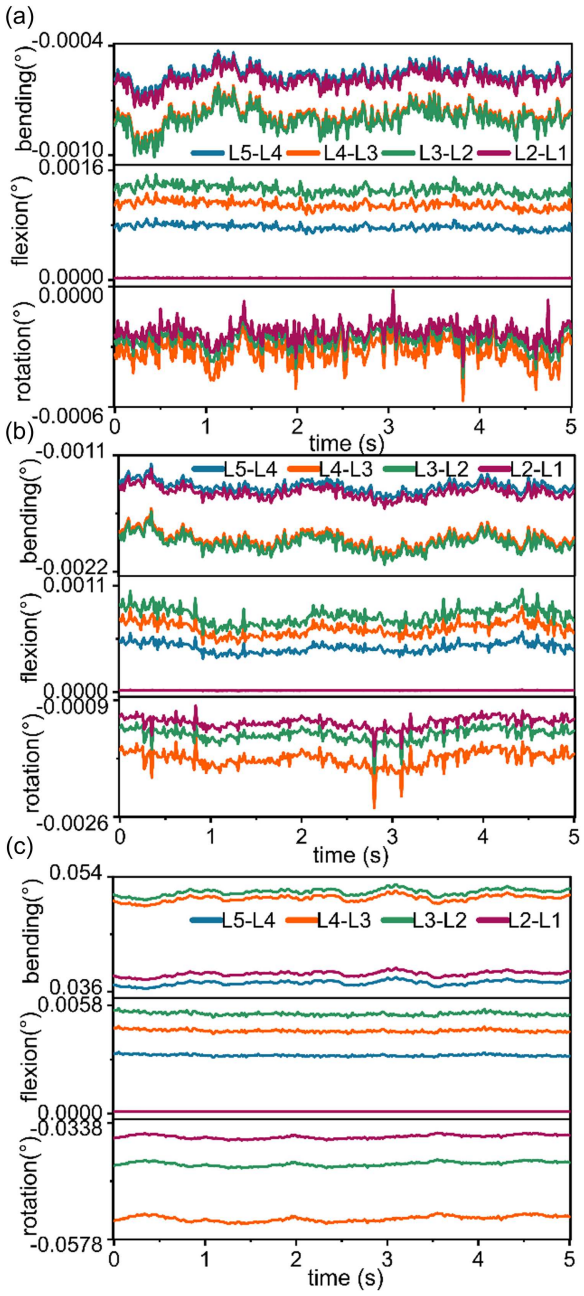

Table S1

Average muscle torque values of lumbar joints under left lateral bridge posture

Lateral_Left			
Lumbar Joint	bendjnt.AVG(N·m)	jnt.AVG(N·m)	rotjnt.AVG(N·m)
L4–L5	72.61	-29.48	6.555
L3–L4	62.90	-25.72	6.551
L2–L3	54.25	-21.92	4.92
L1–L2	46.93	/	3.20

Note: This table characterizes the linear distribution trend of different types of lumbar joint torques under the left lateral bridge posture.

Table S2
Average muscle torque values of lumbar joints under left bird-dog posture (Fly_left)

Fly_Left			
Lumbar Joint	bendjnt.AVG(N·m)	jnt.AVG(N·m)	rotjnt.AVG(N·m)
L4–L5	-39.80	83.40	-2.09
L3–L4	-35.42	74.20	-2.02
L2–L3	-31.53	66.61	-1.24
L1–L2	-28.24	/	-0.45

Note: This table characterizes the linear distribution trend of different types of lumbar joint torques under the left bird-dog posture.

Table S3
Overall average forces exerted by IL and LTpL muscles under lateral bridge posture

	IL		LTpL	
bodyside posture	lateral right	lateral left	lateral right	lateral left
mean.AVG.r(N)	28.4234	29.616	23.653	23.440
mean.AVG.r(N)	26.512	30.443	23.038	23.820

Note: (Right side of Table S3) Torques exerted by bilateral LTpL on lumbar joints under left and right lateral bridge postures.

Detailed Description of Figure 15:

Lateral bridge test:

Figure 15(a) (20–60 Hz frequency band):

For the left posture, highly significant differences ($p < 0.01$) were observed in Subjects 1, 3, and 4, and a significant difference ($p < 0.05$) was found in Subject 2. For the right posture, highly significant differences ($p < 0.01$) appeared in Subjects 1 and 3, a significant difference ($p < 0.05$) in Subject 2, and no significant difference ($p > 0.05$) in the proportional band energy between activated and inactivated states for Subject 4.

Figure 15(b) (90–150 Hz frequency band):

In the left posture, highly significant differences ($p < 0.01$) were detected in Subjects 1 and 2, a significant difference ($p < 0.05$) in Subject 4, and no significant difference ($p > 0.05$) in Subject 3. In the right posture, all subjects (1, 2, 3, and 4) showed highly significant differences ($p < 0.01$).

Bird-dog test:

Figure 15(c) (20–60 Hz frequency band):

In the left posture, highly significant differences ($p < 0.01$) were present in Subjects 1, 3, and 4, and a significant difference ($p < 0.05$) in Subject 2. In the right posture, a highly significant difference ($p < 0.01$) was observed in Subject 4, significant differences ($p < 0.05$) in Subjects 1 and 2, and no significant difference ($p > 0.05$) in Subject 3.

Figure 15(d) (90–150 Hz frequency band):

In both left and right posture tests, all subjects (1, 2, 3, and 4) exhibited highly significant differences ($p < 0.01$).

References

[1] Arts, L. P. A., & van Den Broek, Egon. L. (2022). The fast continuous wavelet transformation (fCWT) for real-time, high-quality, noise-resistant time–frequency analysis. *Nature Computational Science*, *2*(1), 47–58. https://doi.org/10.1038/s43588-021-00183-z

[2] Sarker, P., & Mirka, G. (2019). Effects of sampling frequency and sample window size on median frequency of surface EMG. *Proceedings of the Human Factors and Ergonomics Society Annual Meeting*, *63*(1), 1369–1372. https://doi.org/10.1177/1071181319631166

[3] Gagnat, Y., Brændvik, S. M., &; Roeleveld, K. (2020). Surface electromyography normalization affects the interpretation of muscle activity and coactivation in children with cerebral palsy during walking. *Frontiers in Neurology*, *11*, 202. "https://doi.org/10.3233/THC-191939"

[4] Li, W., Li, Z., Qie, S., Yang, H., Chen, X., Liu, Y., ..., &; Zhang, K. (2020). Analysis of the activation modalities of the lower limb muscles during walking. *Technology and Health Care*, *28*(5), 521–532. https://doi.org/10.3233/THC-191939